International Wound Journal

WILEY

IWJ

ORIGINAL ARTICLE OPEN ACCESS

Pooled, Frozen, Gamma-Irradiated Amniotic Fluid Enhances Histomorphological Remodelling in Hypertrophic Scars

Gamze Tumentemur[1] | Elif Ganime Aygun[2] | Bulut Yurtsever[3] | Ercument Ovali[3]

[1]Vocational School of Health Services, Anatomy, Acibadem Mehmet Ali Aydinlar University, Istanbul, Turkey | [2]Department of Obstetrics and Gynecology, Atakent Hospital, Acibadem Mehmet Ali Aydinlar University, Istanbul, Turkey | [3]Acibadem Labcell Cellular Therapy Laboratory, Istanbul, Turkey

Correspondence: Gamze Tumentemur (gtumentemur.acibadem@gmail.com)

Received: 12 May 2025 | **Revised:** 12 August 2025 | **Accepted:** 15 August 2025

Funding: The authors received no specific funding for this work.

Keywords: gamma irradiation | granulation tissue | human amniotic fluid | hypertrophic scar | regenerative medicine

ABSTRACT

Hypertrophic scars (HTSs) result from excessive collagen accumulation and impaired wound remodelling, leading to considerable aesthetic and functional concerns. Despite the availability of various treatment strategies, their clinical success remains limited, emphasising the need for alternative approaches. Human amniotic fluid (hAF), naturally enriched with cytokines and growth factors, has emerged as a promising biological material for tissue regeneration. This study investigated the therapeutic potential of two forms of hAF—pooled-frozen and pooled-frozen gamma-irradiated—in a rat model of hypertrophic scarring. Fifteen adult male Sprague–Dawley rats were randomly assigned to receive subcutaneous injections of either saline, pooled-frozen hAF, or pooled-frozen gamma-irradiated hAF at the wound margins on days 1, 3 and 5 following the induction of hypertrophic scars via talc powder application. After 21 days, wound healing was evaluated through histological and immunohistochemical analyses. Both treatment groups demonstrated significantly improved wound healing compared to the control group. Granulation tissue formation was enhanced in the treated groups, particularly in animals receiving gamma-irradiated fluid, which also showed superior collagen remodelling characterised by aligned and mature collagen bundles. Both treatment groups demonstrated an increase in M2 macrophage density, as evidenced by elevated $Arg^+/CD68^+$ cell ratios; however, this effect was more pronounced in the gamma-irradiated group, indicating a stronger shift towards a regenerative immune profile. Enhanced reepithelialisation, increased hair follicle density and reduced scar thickness were also observed. These findings suggest that gamma-irradiated hAF provides a more effective and minimally invasive therapeutic option for modulating scar formation and improving wound healing outcomes, supporting its potential translation into clinical applications for the management of hypertrophic scars.

1 | Introduction

Hypertrophic scars are benign, fibroproliferative lesions that arise following deep dermal injuries, such as severe burns, surgical interventions, or traumatic wounds. Characterised by excessive collagen deposition, persistent inflammation, myofibroblast hyperactivity and dermal tissue proliferation, HTSs manifest as raised, visible scars that do not invade surrounding tissues [1–3]. These scars result from aberrant wound healing processes driven by mechanical tension and dysregulated

Abbreviations: AAMI, Association for the Advancement of Medical Instrumentation; Arg^+, arginase-1 positive; $CD68^+$, cluster of differentiation 68 positive; CNT, control; hAF, human amniotic fluid; H&E, haematoxylin and eosin; HTS, hypertrophic scar; ISO, International Organization for Standardization; M1, macrophage 1; M2, macrophage 2; PF-hAF, pooled-frozen human amniotic fluid; PFI-hAF, pooled-frozen gamma-irradiated human amniotic fluid.

Summary

- Gamma-irradiated pooled amniotic fluid accelerates hypertrophic scar remodeling.
- Histomorphology shows reduced fibrosis and improved tissue organization.
- Demonstrates therapeutic potential of processed amniotic fluid in wound healing.

extracellular matrix remodelling [4]. Clinically, HTSs cause cosmetic disfigurement, functional impairment, pruritus and pain, significantly reducing patients' physical, psychological and social quality of life [5]. Consequently, there is a pressing need for innovative therapies that target the pathological mechanisms of HTS to improve both functional and aesthetic outcomes.

Human amniotic fluid offers a promising therapeutic avenue due to its unique regenerative properties observed in scarless foetal wound healing. Rich in growth factors (e.g., TGF-β, VEGF), cytokines and other bioactive molecules, hAF promotes cell migration, proliferation and metabolic activity, creating an optimal environment for tissue repair [6, 7]. In the context of HTSs, hAF's anti-inflammatory properties and ability to modulate myofibroblast activity and collagen organisation may mitigate the fibrotic processes that drive scar pathology [8]. By regulating excessive extracellular matrix deposition and promoting balanced tissue remodelling, hAF has the potential to enhance the histomorphological structure of hypertrophic scars, improving their microscopic architecture and elasticity [9].

Despite its therapeutic potential, the clinical application of fresh hAF is hindered by significant biological and logistical challenges, including the risk of disease transmission, short shelf life and difficulties in storage and transport [10]. Fresh amniotic material, while effective as a temporary skin substitute, poses infection risks that limit its practicality. To address these issues, gamma irradiation provides a standardised and effective sterilisation method that eliminates microbial contamination while preserving the functional integrity of hAF's bioactive components [11]. Freezing further extends shelf life and facilitates long-term storage, overcoming logistical barriers. Pooling hAF from multiple donors ensures consistency in the biochemical and biological composition of the product, enabling standardised clinical applications. Additionally, acellular processing reduces immunogenicity, minimising the risk of adverse immune responses in recipients.

While clinical experience with fresh or cryopreserved amniotic membranes is well-documented, the use of pooled, frozen and gamma-irradiated acellular hAF for hypertrophic scar treatment remains unexplored. This gap in the literature underscores the need for novel approaches to address HTS pathology. In this study, we experimentally evaluate the impact of pooled, frozen and gamma-irradiated acellular amniotic fluid on the histomorphological structure of hypertrophic scar tissue, focusing on its effects on collagen organisation, fibroblast activity and tissue architecture. By addressing this research gap, we aim to provide insights into the potential of processed hAF as a safe and effective therapeutic option for improving hypertrophic scar outcomes.

2 | Materials and Methods

2.1 | Animal Model and Ethical Approval

Wistar Albino rats aged 6–8 weeks were used for animal modelling (female, weighing 200–300 g). Rats were maintained in the animal facility at 23°C–26°C and in a 12-h light/dark cycle with free access to standard food and clean water. Experimental protocols and procedures were approved by the Animal Experimental Management Committee (2019/32). Animals were acclimatised for 7 days prior to the start of the experiment to minimise stress.

HTSs were induced using a talc powder-based model to promote fibrosis and scar formation. Under general anaesthesia with 2%–3% isoflurane (Baxter, Deerfield, IL, USA) delivered via inhalation, the dorsal skin of each rat was shaved and disinfected with 70% ethanol. A 2 cm × 2 cm full-thickness excisional wound was created on the midline of the dorsum using a sterile scalpel. To induce hypertrophic scar formation, 0.5 g of sterile talc powder (USP grade, Sigma-Aldrich, St. Louis, MO, USA) was evenly applied to the wound bed immediately after excision in order to stimulate chronic inflammation and fibrosis.

2.2 | Preparation of Human Amniotic Fluid

hAF was collected from healthy, consenting donors undergoing elective caesarean sections. Donors were screened for infectious diseases, including HIV, hepatitis B and C and syphilis, to ensure safety. Amniotic fluid was aspirated under sterile conditions during caesarean delivery and immediately processed.

2.3 | Pooled-Frozen hAF (PF-hAF)

Collected hAF samples from multiple donors were pooled to create a standardised product with consistent biochemical composition. The pooled hAF was centrifuged at 1000 *g* for 10 min at 4°C to remove cellular debris, resulting in acellular hAF. The supernatant was filtered through a 0.22 μm sterile filter (MilliporeSigma, Burlington, MA, USA) to ensure sterility. The filtered hAF was aliquoted into 2 mL cryogenic vials and stored at −80°C until use. Prior to administration, PF-hAF was thawed at 37°C in a water bath and used within 1 h to preserve bioactivity.

2.4 | Pooled-Frozen Gamma-Irradiated hAF (PFI-hAF)

A portion of the pooled, filtered hAF was subjected to gamma irradiation for additional sterilisation. Aliquots were irradiated at a dose of 25 kGy at a certified irradiation facility, following established standards for tissue sterilisation [12, 13]. Irradiated samples were stored at −80°C and thawed identically to PF-hAF before use. The irradiation process was validated to eliminate microbial contamination while preserving the functional integrity of growth factors and cytokines, as confirmed by enzyme-linked immunosorbent assay (ELISA) for key bioactive molecules (e.g., TGF-β, VEGF) [14].

2.5 | Experimental Design

Rats were randomly assigned to three groups ($n = 5$ per group) using a randomisation sequence:

Control Group (CNT): Rats received 1 cc of sterile normal saline (0.9% NaCl, Hospira, Lake Forest, IL, USA) administered subcutaneously at the wound margins on days 1, 3 and 5 post-injury.

Pooled-Frozen hAF Group (PF-hAF): Rats received 1 cc of PF-hAF administered subcutaneously at the wound margins on days 1, 3 and 5 post-injury.

Pooled-Frozen Gamma-Irradiated hAF Group (PFI-hAF): Rats received 1 cc of PFI-hAF administered subcutaneously at the wound margins on days 1, 3 and 5 post-injury.

2.6 | Sample Collection

On day 21 post-injury, rats were euthanised under deep anaesthesia induced by intraperitoneal administration of xylazine (10 mg/kg) and ketamine (90 mg/kg), followed by exsanguination via cardiac puncture. Scar tissue, including a 5 mm margin of surrounding healthy skin, was excised using a sterile scalpel. Tissue samples were immediately fixed in 10% neutral buffered formalin (Sigma-Aldrich, St. Louis, MO, USA) for 24 h at room temperature for histological analysis.

2.7 | Histological Analysis

Fixed scar tissue samples were dehydrated through a graded ethanol series, cleared in xylene and embedded in paraffin. Serial sections (5 μm thick) were cut using a microtome (Leica RM2235, Leica Biosystems, Wetzlar, Germany) and mounted on glass slides. Sections were stained with haematoxylin and eosin (H&E) for general morphology and Masson's trichrome for collagen fibre assessment, following standard protocols.

2.8 | Scar Thickness

Scar thickness was measured as the maximum vertical distance from the epidermal surface to the deepest point of the scar tissue in H&E-stained sections. Measurements were taken at three random fields per section, with three sections per animal, using a calibrated light microscope (Olympus BX51, Olympus, Tokyo, Japan) equipped with image analysis software (ImageJ, NIH, Bethesda, MD, USA).

2.9 | Granulation Tissue Formation

Granulation tissue was evaluated in H&E-stained sections by assessing the extent of new blood vessel formation, inflammatory cell infiltration and fibroblast density. A semi-quantitative scoring system (0 = absent, 1 = mild, 2 = moderate and 3 = severe) was used by two blinded investigators to ensure objectivity.

2.10 | Fibrosis

Fibrosis was quantified in Masson's trichrome-stained sections by measuring the intensity and organisation of collagen fibres. Collagen fibre density was assessed using ImageJ to calculate the percentage of blue-stained collagen relative to the total tissue area in three random fields per section. Fibre organisation was evaluated qualitatively for alignment and bundling patterns, with disorganised fibres indicating higher fibrosis.

2.11 | Macrophage Subtype Infiltration

Immunohistochemistry (IHC) was performed to assess macrophage subtype infiltration (M1 and M2). Sections were deparaffinised, rehydrated and subjected to antigen retrieval using citrate buffer (pH 6.0) at 95°C for 20 min. Endogenous peroxidase activity was blocked with 3% hydrogen peroxide. Sections were incubated with primary antibodies against CD68 (M1 marker, 1:100, Abcam) and Arginase 1 (M2 marker, 1:150, Abcam) overnight at 4°C. Secondary antibodies conjugated with horseradish peroxidase (1:500, Dako, Glostrup, Denmark) were applied, followed by visualisation with 3,3′-diaminobenzidine (DAB, Dako). Sections were counterstained with haematoxylin. Positive cells were quantified in three random high-power fields (400× magnification) per section using ImageJ and the M1/M2 ratio was calculated to assess inflammatory modulation.

2.12 | Statistical Analysis

Data were analysed using GraphPad Prism version 9.0 (GraphPad Software, San Diego, CA, USA). Normality was assessed with the Shapiro–Wilk test. Scar thickness, collagen density and macrophage counts were compared across groups using one-way analysis of variance (ANOVA) followed by Tukey's post hoc test for normally distributed data, or the Kruskal–Wallis test with Dunn's post hoc test for non-parametric data. Granulation tissue scores were analysed using the Kruskal–Wallis test. Results are presented as mean ± standard deviation (SD) for parametric data or median (interquartile range) for non-parametric data. A p-value < 0.05 was considered statistically significant.

3 | Results

A HTSs model was successfully established in all rats by day 21 following talc powder application, as evidenced by elevated, irregular scar tissue (Figure 1). On day 21, biopsy samples were collected from the CNT, PF-hAF and PFI-hAF groups (Figure 2A) for macro-morphological (Figure 2B) and histological evaluations (Figure 3A).

3.1 | Macro-Morphological Findings

Figure 2A schematically represents the experimental timeline, indicating the initiation of the hypertrophic scar model

on day 0 and euthanasia on day 21. Although not shown in the schematic, subcutaneous treatments were administered at the wound margins on days 1, 3 and 5. The CNT group exhibited prominent hypertrophic scarring, characterised by raised, erythematous and irregular scar tissue (Figure 2B). In contrast, the PF-hAF-treated group showed significant scar resolution, with reduced elevation and smoother surface texture. The PFI-hAF-treated group demonstrated the most pronounced improvement, with near-complete resolution of hypertrophic scarring, presenting a flatter, less erythematous scar surface closely resembling normal skin (Figure 2B). By day 21, the hypertrophic scar areas in the PF-hAF- and especially PFI-hAF-treated groups exhibited near-complete HTS resolution, whereas the CNT group retained noticeable scars (Figure 2B).

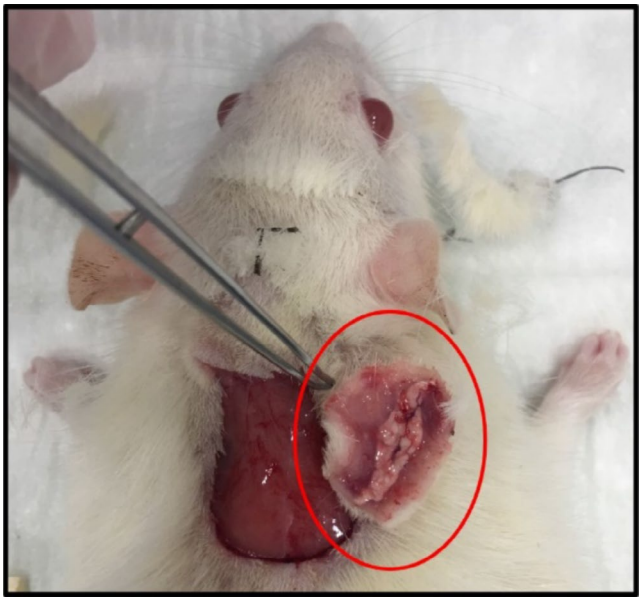

FIGURE 1 | Hypertrophic scar model in a rat on day 21. The red-circled area highlights the HTS tissue, appearing elevated and irregular, characteristic of hypertrophic scars.

3.2 | Histological Analyses

Histological evaluation using haematoxylin and eosin (H&E), Masson's trichrome and immunohistochemistry provided detailed insights into the histomorphological changes in scar tissue (Figure 3A).

3.3 | Reepithelialisation and Hair Follicle Migration

In the CNT group, H&E-stained sections revealed an irregular dermal matrix with increased fibrotic tissue, dense inflammatory cell infiltration and a lack of hair follicles, glandular structures and sweat glands in the subdermal wound areas. In contrast, the PF-hAF and PFI-hAF groups showed significant reepithelialisation and keratinisation, with a marked increase in hair follicle density within areas typically responsible for fibrotic scar development. Hair follicles were observed migrating from the hypodermis to the subdermis, with this progression being more evident in the PFI-hAF group (Figure 3A). Granulation tissue, a critical indicator of wound healing, was significantly increased in the PF-hAF and PFI-hAF groups compared to the CNT group. H&E-stained sections showed a median granulation tissue in the CNT group, indicating persistent fibrotic activity (Figure 3A). In contrast, the PF-hAF group ($p < 0.01$ vs. CNT) and the PFI-hAF group ($p < 0.01$ vs. CNT, $p < 0.05$ vs. PF-hAF) suggested accelerated wound healing and reduced fibrosis. The PFI-hAF group exhibited a more dramatic healing trend, with minimal residual granulation tissue and enhanced tissue remodelling (Figure 3B). Quantitative analysis of granulation tissue area per healed wound revealed a significant increase in both PF-hAF ($p < 0.01$ vs. CNT) and PFI-hAF ($p < 0.01$ vs. CNT) groups compared to the control, indicating enhanced early wound healing response and fibroblast activation. Furthermore, analysis of hair follicle density showed a statistically significant increase in the PF-hAF ($p < 0.003$ vs. CNT) and PFI-hAF ($p < 0.0001$ vs. CNT) groups, with the PFI-hAF group exhibiting the highest density (Figure 3B–D).

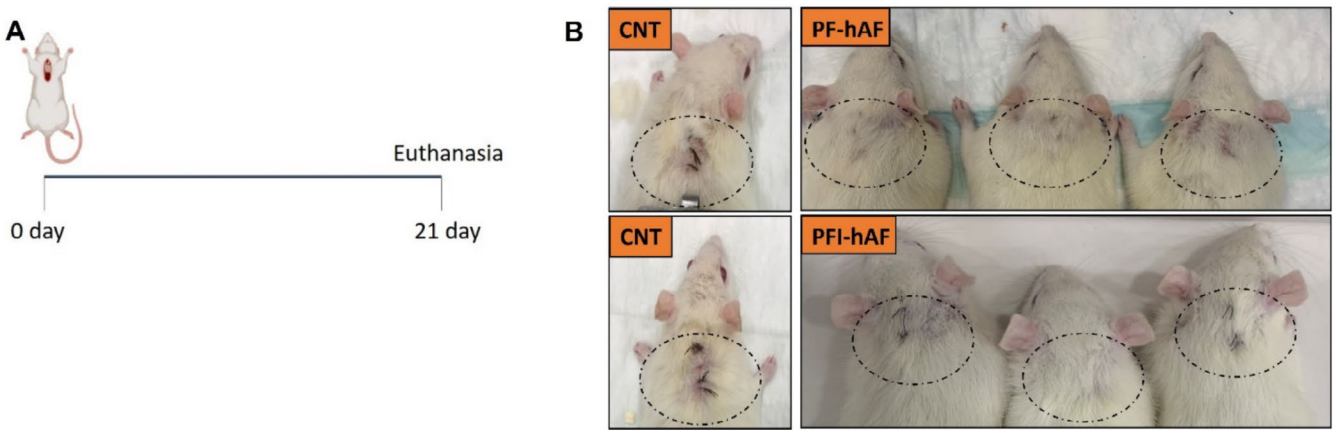

FIGURE 2 | Results showing recovery and wound healing in the rat groups: (A) A schematic representation of the study where the HTSs model was established on the dorsal region of the rats. Treatments (CNT, PF-hAF and PFI-hAF) were administered via intraperitoneal injection on days 1, 3 and 5. (B) The healing process of hypertrophic scars in different groups is visually displayed, demonstrating distinct changes in scar morphology, with prominent scarring in the CNT group, partial resolution in the PF-hAF group and near-complete resolution in the PFI-hAF group.

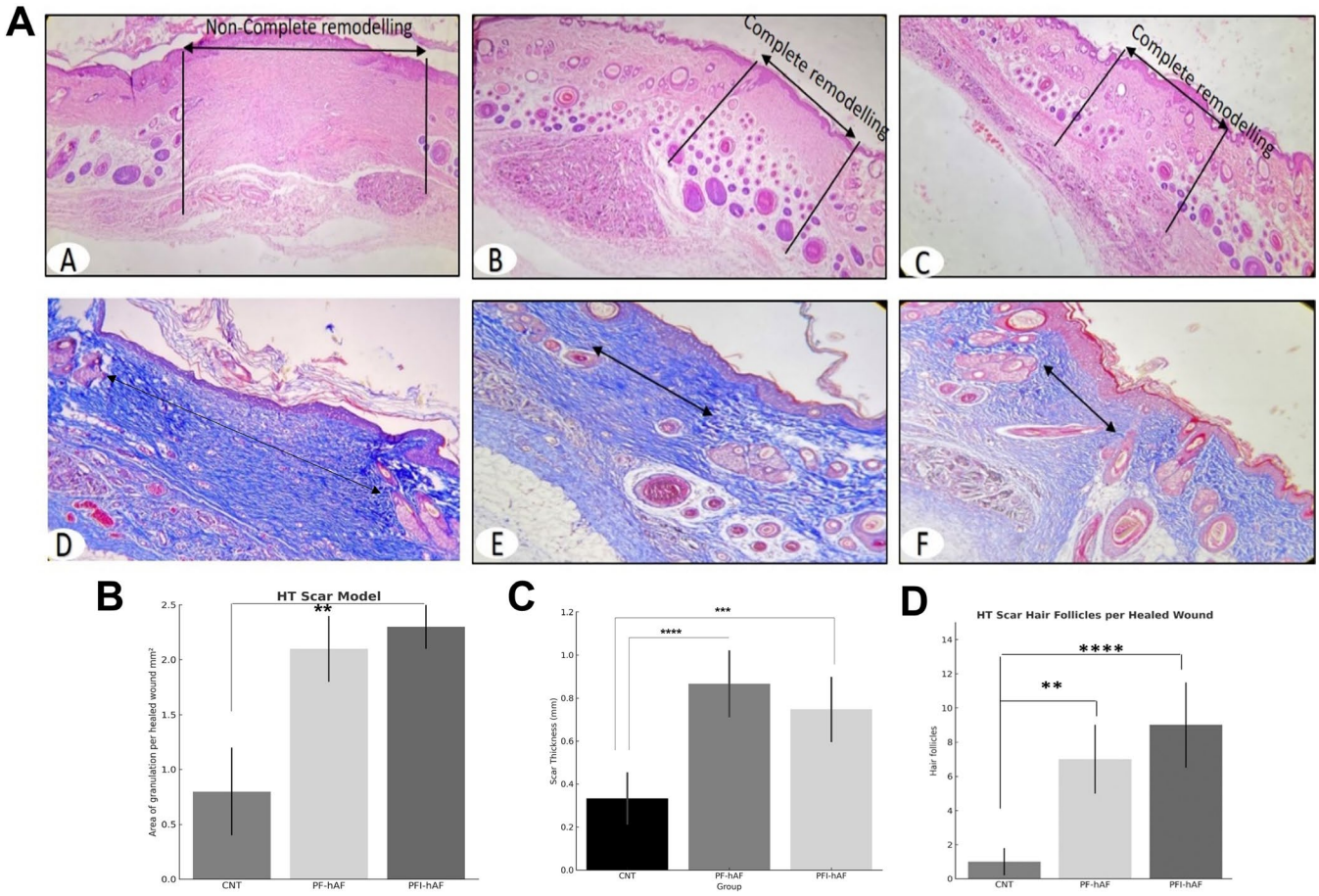

FIGURE 3 | Histological and quantitative evaluation of wound healing in the hypertrophic scar model. (A) Representative histological images of scar tissue on day 21 from the CNT (A, D), PF-hAF (B, E) and PFI-hAF (C, F) groups. Upper row (A–C): Haematoxylin and eosin (H&E) staining demonstrating incomplete (A) and complete dermal remodelling with organised skin appendages (B, C). Lower row (D–F): Masson's trichrome staining showing dense and disorganised collagen fibres in the CNT group (D), compared to more structured and aligned collagen bundles in both treatment groups (E, F). Scale Bar: 400 μm for both H&E and Masson's trichrome. (B) Quantitative assessment of granulation tissue area per healed wound. Both PF-hAF and PFI-hAF groups showed significantly higher granulation tissue area compared to the control ($p < 0.01$). (C) Scar thickness was significantly greater in both PF-hAF and PFI-hAF groups compared to CNT ($p < 0.0001$ and $p < 0.001$, respectively), suggesting enhanced early healing responses. (D) Hair follicle density per healed wound area. Both treatment groups showed significantly increased follicle numbers compared to CNT ($p < 0.01$ for PF-hAF, $p < 0.0001$ for PFI-hAF), with the PFI-hAF group displaying the highest density.

3.4 | Comparison of Scar Thickness Between Groups

Scar thickness was significantly higher in both treatment groups compared to the control group ($p = 0.0001$ for PF-hAF vs. CNT; $p = 0.0007$ for PFI-hAF vs. CNT), indicating the presence of robust early granulation tissue formation in response to hAF administration. However, no statistically significant difference was observed between the PF-hAF and PFI-hAF groups ($p = 0.234$), suggesting that while both treatments effectively modulated wound architecture, their impact on scar thickness was comparable (Figure 3C).

3.5 | Granulation Tissue Scoring Table

Semi-quantitative histological scoring of granulation tissue formation in different treatment groups. Scoring was based on the extent of new blood vessel formation, inflammatory cell infiltration and fibroblast density in H&E-stained sections. Two blinded investigators independently evaluated each sample using a scale from 0 to 3 (0 = absent, 1 = mild, 2 = moderate and 3 = severe) (Table 1).

3.6 | Collagen Accumulation

Masson's trichrome staining demonstrated significant improvements in collagen organisation in the treatment groups compared to the CNT group. In the CNT group, collagen fibres were densely packed, disorganised and haphazardly arranged, indicative of excessive fibrosis. The PF-hAF group showed reduced collagen density and improved fibre alignment, with more parallel and evenly distributed fibres (Figure 3A).

3.7 | The Role of Arginase-1 and CD68

Arg-1 played a dominant role in fibrosis regulation, while CD68 served as a critical but complementary factor during

the wound healing process. Immunohistochemical staining revealed minimal expression of both CD68 and Arg-1 in the CNT group, consistent with limited regenerative activity. In the PF-hAF and PFI-hAF groups, a significant increase in both CD68 and Arg-1 expression was detected ($p < 0.01$ vs. CNT for both markers). The PFI-hAF group exhibited the highest Arg-1 expression, particularly surrounding hair follicles in the subdermal and dermal regions, indicating successful regeneration of structural components (Figure 4A). The PF-hAF group also showed elevated Arg-1 expression, but to a lesser extent than PFI-hAF ($p < 0.05$ vs. PFI-hAF). These findings highlight the enhanced regenerative capacity of PFI-hAF in modulating fibrosis and promoting tissue remodelling. Specifically, CD68 expression, indicating total macrophage infiltration, was significantly higher in the PF-hAF and PFI-hAF groups, with the rate of CD68+ cells in the HTS model increasing from the CNT group to the PF-hAF group ($p < 0.01$ vs. CNT) and the PFI-hAF group ($p < 0.001$ vs. CNT, $p < 0.01$ vs. PF-hAF, Figure 4B).

TABLE 1 | Semi-quantitative histological scoring of granulation tissue formation in different treatment groups.

Group	Granulation tissue score (mean ± SD)	Statistical significance (vs. control)
Control	0.8 ± 0.4	—
PF-hAF	2.1 ± 0.3	$p < 0.01$
PFI-hAF	2.3 ± 0.2	$p < 0.01$

4 | Discussion

hAF has garnered significant attention for its potential in wound healing, primarily due to the action of mesenchymal stem cells (MSCs), growth factors and other regenerative mechanisms [15–18]. Unlike other stem cell-based therapies, minimally manipulated hAF is not subject to the same ethical and legal restrictions, making it a promising candidate for clinical applications [19]. This is particularly relevant given the growing demand for ethical, accessible and non-invasive wound healing treatments. In our study, we demonstrated that hAF, when immediately pooled, frozen and gamma-irradiated (PFI-hAF), has a direct and significant impact on HTS wound healing. Unlike previous studies focusing on complex stem cell-based treatments, our research highlights that PFI-hAF, in its pure, pooled and irradiated form, acts as a minimally manipulated product while effectively promoting tissue repair. This finding positions PFI-hAF as a sustainable and practical solution for clinical wound care, requiring minimal processing and offering convenient storage options, such as room-temperature stability for dried forms.

Our approach aligns with prior efforts to enhance the safety and usability of amniotic products. For instance, Nakamura et al. developed a sterilised, freeze-dried amniotic membrane using

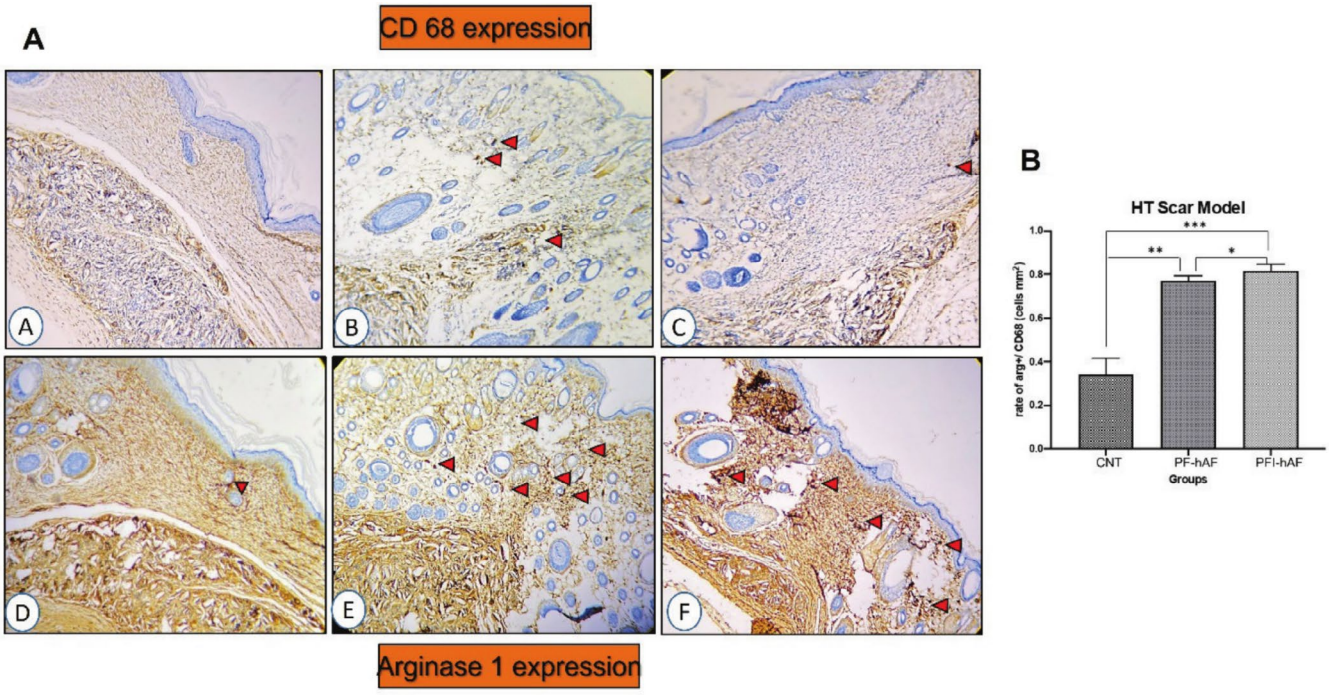

FIGURE 4 | CD68 and Arginase-1 expression in wound healing tissue: (A) Immunohistochemical staining of CD68 (upper row: A, B, C) and Arginase-1 (lower row: D, E, F) in the HTS tissue of the CNT, PF-hAF and PFI-hAF groups, respectively. Red arrowheads indicate positive staining for macrophages (CD68) and M2 macrophages (Arginase-1). (A—A, A—D) CNT group: Minimal CD68 and Arg-1 expression. (A—B, A—E) PF-hAF group: Increased CD68 and Arg-1 expression. (A—C, A—F) PFI-hAF group: Highest CD68 and Arg-1 expression, particularly surrounding hair follicles, indicating successful regeneration. (B) Quantification of Arg+/CD68+ cells macrophage density in healed wound tissues CNT, PF-hAF ($p < 0.01$ vs. CNT) and PFI-hAF ($p < 0.001$ vs. CNT, $p < 0.05$ vs. PF-hAF).

a special vacuum-packaging process combined with gamma irradiation, addressing sterilisation and preservation challenges [20, 21]. Similarly, studies from India have explored fresh amnion [22–24] or amnion preserved in antibiotic solutions [22, 25], while Rehni et al. [26] investigated dried amniotic membranes for burn wound care. Our study expands on these concepts by demonstrating that dried amniotic fluid—rather than just the amniotic membrane—can effectively treat scars, including HTS. The ability of dried amniotic fluid to be stored at room temperature simplifies logistics and long-term storage, a key advantage over fresh or non-irradiated forms. Moreover, pooled amniotic fluid enhances safety and reliability by offering protection against viral and pyrogenic contamination. Non-sterilised amniotic fluid poses significant risks of fungal, bacterial, or viral infections from the donor, emphasising the clinical relevance of gamma-irradiated hAF. To date, few studies have investigated the clinical efficacy of gamma-irradiated amniotic membranes [27], and only one study has specifically examined gamma-irradiated amniotic fluid [14]. Our findings build on this limited body of work, providing novel evidence of PFI-hAF's efficacy in HTS management.

In foetal tissues, skin regeneration occurs without scarring due to a diminished inflammatory response, attributed to differences in the size and maturity of macrophages, neutrophils and mast cells compared to adult tissues [28]. Macrophages, key regulators of immune responses and tissue repair, are classified into M1 (pro-inflammatory) and M2 (pro-regenerative) subtypes, though they exist along a continuum of intermediate states. M1 macrophages, induced by bacterial metabolites, interferon-gamma (IFN-γ), or granulocyte-macrophage colony-stimulating factor (GM-CSF), secrete pro-inflammatory cytokines and phagocytose dead cells and pathogens [29]. In contrast, M2 macrophages, activated by interleukin-13 (IL-13) and/or interleukin-4 (IL-4) [30], promote tissue repair by secreting anti-inflammatory cytokines and angiogenic factors, facilitating scarless tissue closure [29]. Our study found that PFI-hAF significantly enhanced M2 macrophage activity, as evidenced by the lowest M1/M2 ratio and the highest Arg+/CD68+ cell density. These results align with Tumentemur et al. [14], which demonstrated that gamma-irradiated amniotic fluid enhances M2 macrophage activation, promotes tissue regeneration and modulates inflammation. The shift from M1 to M2 macrophages in the PFI-hAF group likely contributes to the observed reduction in granulation tissue by day 21, reflecting a more advanced healing stage with reduced fibrotic activity. Histologically, this reduction in granulation tissue suggests a faster transition from the proliferative phase to the remodelling phase, potentially due to decreased angiogenesis and accelerated extracellular matrix maturation, which are hallmarks of scar resolution in HTS [31]. This mirrors foetal wound healing dynamics and suggests that PFI-hAF may partially recapitulate scarless healing mechanisms in adult tissues.

Our analysis revealed that PFI-hAF significantly enhanced re-epithelialisation compared to PF-hAF, with no such effect in control wounds. Re-epithelialisation, a crucial component of wound healing, occurs at the edges of full-thickness wounds and contributes to epidermal restoration, ensuring proper wound closure through submarginal thickening and tissue remodelling [32]. Impaired re-epithelialisation can lead to chronic wounds or abnormal scarring [33]. Compared to amniotic fluid-derived stem cells (AFSC), amniotic fluid itself appears to play a more prominent role in the early stages of wound healing [34]. Our findings highlight PFI-hAF's ability to promote complete wound healing and improve scar tissue quality, as evidenced by increased hair follicle density and reduced scar width. Histologically, the enhanced re-epithelialisation in the PFI-hAF group, coupled with increased hair follicle migration, indicates a restoration of normal dermal architecture, which is critical for functional and aesthetic outcomes in HTS healing. The presence of hair follicles in the subdermal and dermal regions suggests a regenerative process akin to foetal wound healing, where appendage regeneration contributes to scarless repair [35]. This finding underscores PFI-hAF's potential to not only close wounds but also regenerate skin appendages, a key differentiator from traditional scar treatments. The reduction in granulation tissue area following PFI-hAF treatment indicates an accelerated transition to the remodelling phase, consistent with prior studies like Fukutake et al. [15], which demonstrated amniotic fluid's wound-healing-promoting effects.

HTS formation reflects the remodelling phase of wound healing, where collagen synthesis occurs alongside the degradation of vascular and cellular components. An imbalance between collagen production and degradation can lead to excessive deposition and irregular scar formation. Amniotic membranes are a potent source for wound healing due to their rich content of MSCs, collagen matrices and growth factors [36]. In our study, the control group exhibited collagen accumulation and irregular collagen bundles, while PF-hAF and PFI-hAF-treated wounds displayed thicker collagen fibres with regular borders, aligned parallel to the epidermis. PFI-hAF resulted in the most organised collagen structure and the greatest reduction in granulation tissue area, suggesting that gamma irradiation enhances hAF's therapeutic properties by optimising collagen remodelling and improving scar quality. This finding is consistent with Yang et al. [34], which showed that amniotic fluid promotes well-organised collagen bundles and facilitates wound closure. The improved collagen organisation likely results from growth factors in hAF, such as transforming growth factor-beta (TGF-β) and epidermal growth factor (EGF), which regulate fibroblast activity and extracellular matrix deposition [37]. Histologically, the transition to thicker, more parallel collagen bundles in the PFI-hAF group not only enhances scar quality but also likely improves the biomechanical properties of the healed tissue, such as tensile strength and elasticity, which are critical for preventing contractures and improving patient outcomes [38]. The reduced collagen density in treated groups further suggests a balanced remodelling process, minimising the risk of excessive fibrosis, which is a common challenge in HTS management.

The mechanisms underlying PFI-hAF's efficacy likely involve macrophage modulation and the action of growth factors. Macrophages phagocytize pathogens, matrix debris and necrotic tissue, while also regulating the progression to fibrosis [39–43]. In our study, PFI-hAF increased M2 macrophage activity, suggesting a regenerative response, though high CD68 expression indicates an ongoing inflammatory phase. This balance suggests that PFI-hAF enhances the transition from inflammation to regeneration, aligning with studies emphasising macrophage phenotypes in tissue repair [44, 45]. Histologically, the increased M2 macrophage activity likely contributes to the observed

improvements in collagen organisation and granulation tissue resolution, as M2 macrophages are known to secrete matrix metalloproteinases (MMPs) and tissue inhibitors of metalloproteinases (TIMPs) that regulate extracellular matrix remodelling [46]. This interplay between macrophage phenotype and histological outcomes underscores the multifaceted role of PFI-hAF in promoting a regenerative microenvironment. Previous research has shown that monocytes and macrophages in amniotic fluid are of foetal origin [47–49] and Lopez et al. [50] found these cells abundant in the chorioamniotic membrane but absent in the umbilical cord. Our findings, combined with Tumentemur et al. [14], suggest that hAF may directly influence macrophage phenotype, potentially shifting Th1 to Th2 responses, which could further modulate immune responses in wound healing.

In conclusion, our study supports the use of irradiated hAF as an effective and minimally manipulated therapeutic option for enhancing wound healing, reducing scarring and improving the overall appearance of scars. The potential for hAF in wound care, especially in clinical settings, is immense and further studies are warranted to optimise its application and ensure its broad clinical efficacy. By integrating PFI-hAF into regenerative medicine strategies, such as combination therapies with bioengineered scaffolds or growth factor-enriched dressings, we may further enhance its therapeutic impact, offering a novel approach to scarless healing in adults.

Acknowledgements

The authors would like to thank the (Acibadem University Animal Research Facility/Animal Laboratory DEHAM) for their support with the animal procedures.

Ethics Statement

Experimental protocols and procedures were approved by the Animal Experimental Management Committee of Acibadem Mehmet Ali University (2019/32).

Conflicts of Interest

The authors declare no conflicts of interest.

Data Availability Statement

The datasets generated during the current study are available from the corresponding author on reasonable request.

References

1. H. J. Lee and Y. J. Jang, "Recent Understandings of Biology, Prophylaxis and Treatment Strategies for Hypertrophic Scars and Keloids," *International Journal of Molecular Sciences* 19, no. 3 (2018): 711.

2. B. S. Atiyeh, "Nonsurgical Management of Hypertrophic Scars: Evidence-Based Therapies, Standard Practices, and Emerging Methods," *Aesthetic Plastic Surgery* 31, no. 5 (2007): 468–492.

3. K. C. Rustad, V. W. Wong, and G. C. Gurtner, "The Role of Focal Adhesion Complexes in Fibroblast Mechanotransduction During Scar Formation," *Differentiation* 86 (2013): 87–91.

4. A. J. Singer, J. E. Hollander, and J. V. Quinn, "Evaluation and Management of Traumatic Lacerations," *New England Journal of Medicine* 337 (1997): 1142–1148.

5. Y. Li, J. Zhang, J. Shi, et al., "Exosomes Derived From Human Adipose Mesenchymal Stem Cells Attenuate Hypertrophic Scar Fibrosis by miR-192-5p/IL-17RA/Smad Axis," *Stem Cell Research & Therapy* 12 (2021): 221.

6. C. C. Yates, P. Hebda, and A. Wells, "Skin Wound Healing and Scarring: Fetal Wounds and Regenerative Restitution," *Birth Defects Research. Part C, Embryo Today* 96, no. 4 (2012): 325–333.

7. R. G. Frykberg and J. Banks, "Challenges in the Treatment of Chronic Wounds," *Advances in Wound Care* 4, no. 9 (2015): 560–582.

8. S. Gutiérrez-Moreno, M. Alsina-Gibert, L. Sampietro-Colom, S. Pedregosa-Fauste, and P. Ayala-Blanco, "Estudio Coste-Beneficio Del Trasplante de Membrana Amniótica Para Úlceras Venosas de Extremidades Inferiores," *Actas Dermo-Sifiliográficas* 102, no. 4 (2011): 284–288.

9. S. Werner and R. Grose, "Regulation of Wound Healing by Growth Factors and Cytokines," *Physiological Reviews* 83, no. 3 (2003): 835–870.

10. T. Nakamura, E. Sekiyama, M. Takaoka, et al., "The Use of Trehalose-Treated Freeze-Dried Amniotic Membrane for Ocular Surface Reconstruction," *Biomaterials* 29, no. 27 (2008): 3729–3737.

11. G. O. Phillips, "Radiation Technology in Surgery and the Pharmaceutical Industry: An Overview of Applications," *IAEA Bulletin* 36 (1994): 19–23.

12. ANSI/AAMI ST34, *Guideline for the Use of Ethylene Oxide and Steam Biological Indicators in Industrial Sterilization Processes* (ANSI, 1991).

13. ISO 11137, *Sterilization of Health Care Products—Requirements for Validation and Routine Control—Radiation Sterilization* (ISO, 1994).

14. G. Tumentemur, E. G. Aygun, B. Yurtsever, D. Cakirsoy, and E. Ovali, "Effect of Amniotic Fluid on Hair Follicle Growth," *Journal of Dermatological Treatment* 36, no. 1 (2025): 2451389.

15. M. Fukutake, D. Ochiai, H. Masuda, et al., "Human Amniotic Fluid Stem Cells Have a Unique Potential to Accelerate Cutaneous Wound Healing With Reduced Fibrotic Scarring," *Human Cell* 32 (2018): 51–63.

16. B. S. Yoon, J. H. Moon, E. K. Jun, et al., "Secretory Profiles and Wound Healing Effects of Human Amniotic Fluid-Derived Mesenchymal Stem Cells," *Stem Cells and Development* 19 (2010): 887–902.

17. A. Skardal, D. Mack, E. Kapetanovic, et al., "Bioprinted Amniotic Fluid-Derived Stem Cells Accelerate Healing of Large Skin Wounds," *Stem Cells Translational Medicine* 1 (2012): 792–802.

18. V. Castelli, I. Antonucci, M. D'angelo, et al., "Neuroprotective Effects of Human Amniotic Fluid Stem Cells-Derived Secretome in an Ischemia/Reperfusion Model," *Stem Cells Translational Medicine* 10 (2020): 251–266.

19. S. P. Loukogeorgakis and P. De Coppi, "Stem Cells From Amniotic Fluid–Potential for Regenerative Medicine," *Best Practice & Research. Clinical Obstetrics & Gynaecology* 31 (2016): 45–57.

20. T. Nakamura, M. Yoshitani, H. Rigby, et al., "Sterilized, Freeze-Dried Amniotic Membrane: A Useful Substrate for Ocular Surface Reconstruction," *Investigative Ophthalmology & Visual Science* 45, no. 1 (2004): 93–99.

21. T. Nakamura, T. Inatomi, E. Sekiyama, L. P. K. Ang, N. Yokoi, and S. Kinoshita, "Novel Clinical Application of Sterilized, Freeze-Dried Amniotic Membrane to Treat Patients With Pterygium," *Acta Ophthalmologica Scandinavica* 84, no. 3 (2006): 401–405.

22. R. Sinha, "Amniotic Membrane in the Treatment of Burn Injury," *Indian Journal of Surgery* 52 (1990): 11–17.

23. M. Subrahmanyam, "Honey-Impregnated Gauze Versus Amniotic Membrane in the Treatment of Burns," *Burns* 20, no. 4 (1994): 331–333.

24. M. Subrahmanyam, "Amniotic Membrane as a Cover for Microskin Grafts," *British Journal of Plastic Surgery* 48, no. 7 (1995): 477–478.

25. C. V. Bapat and P. M. Kothary, "Preliminary Report on Acceleration of Wound Healing by Amnion Membrane Graft," *Indian Journal of Medical Research* 62, no. 9 (1974): 1342–1346.

26. A. K. Rehni, N. Singh, A. S. Jaggi, and M. Singh, "Amniotic Fluid Derived Stem Cells Ameliorate Focal Cerebral Ischaemia-Reperfusion Injury Induced Behavioural Deficits in Mice," *Behavioural Brain Research* 183 (2007): 95–100.

27. R. Singh, S. Purohit, M. P. Chacharkar, P. S. Bhandari, and A. S. Bath, "Microbiological Safety and Clinical Efficacy of Radiation Sterilized Amniotic Membranes for Treatment of Second-Degree Burns," *Burns* 33 (2007): 505–510.

28. M. Takeo, W. Lee, and M. Ito, "Wound Healing and Skin Regeneration," *Cold Spring Harbor Perspectives in Medicine* 5 (2015): a023267.

29. F. Xu, C. Zhang, and D. T. Graves, "Abnormal Cell Responses and Role of TNF-α in Impaired Diabetic Wound Healing," *BioMed Research International* 2013 (2013): 754802.

30. C. Qing, "The Molecular Biology in Wound Healing & Non-Healing Wound," *Chinese Journal of Traumatology* 20 (2017): 189–193.

31. P. Martin and S. J. Leibovich, "Inflammatory Cells During Wound Repair: The Good, the Bad and the Ugly," *Trends in Cell Biology* 15, no. 11 (2005): 599–607.

32. R. Bryant and D. Nix, *Acute and Chronic Wounds: Current Management Concepts*, 4th ed. (Mosby, 2011).

33. C. Sussman and B. M. Bates-Jensen, *Wound Care: A Collaborative Practice Manual for Health Professionals*, 4th ed. (Lippincott Williams & Wilkins, 2007).

34. J. D. Yang, D. S. Choi, Y. K. Cho, et al., "Effect of Amniotic Fluid Stem Cells and Amniotic Fluid Cells on the Wound Healing Process in a White Rat Model," *Archives of Plastic Surgery* 40 (2013): 496–504.

35. M. Ito, Z. Yang, T. Andl, et al., "Wnt-Dependent de Novo Hair Follicle Regeneration in Adult Mouse Skin After Wounding," *Nature* 447, no. 7142 (2007): 316–320.

36. G. W. Gibbons, "Grafix, a Cryopreserved Placental Membrane, for the Treatment of Chronic/Stalled Wounds," *Advances in Wound Care* 4, no. 9 (2015): 534–544.

37. A. J. Singer and R. A. F. Clark, "Cutaneous Wound Healing," *New England Journal of Medicine* 341, no. 10 (1999): 738–746.

38. D. T. Corr, C. L. Gallant-Behm, N. G. Shrive, and D. A. Hart, "Biomechanical Behavior of Scar Tissue and Uninjured Skin in a Porcine Model," *Wound Repair and Regeneration* 28, no. 2 (2020): 216–225.

39. P. Martin, "Wound Healing–Aiming for Perfect Skin Regeneration," *Science* 276 (1997): 75–81.

40. K. J. Sonnemann and W. M. Bement, "Wound Repair: Toward Understanding and Integration of Single-Cell and Multicellular Wound Responses," *Annual Review of Cell and Developmental Biology* 27 (2011): 237–263.

41. M. Hesketh, K. B. Sahin, Z. E. West, and R. Z. Murray, "Macrophage Phenotypes Regulate Scar Formation and Chronic Wound Healing," *International Journal of Molecular Sciences* 18, no. 7 (2017): 1545.

42. J. Lichtnekert, T. Kawakami, W. C. Parks, and J. S. Duffield, "Changes in Macrophage Phenotype as the Immune Response Evolves," *Current Opinion in Pharmacology* 13, no. 4 (2013): 555–564.

43. T. A. Wynn and K. M. Vannella, "Macrophages in Tissue Repair, Regeneration, and Fibrosis," *Immunity* 44 (2016): 450–462.

44. J. L. V. Eps, C. Boada, J. C. Scherba, et al., "Amniotic Fluid Allograft Enhances the Host Response to Ventral Hernia Repair Using Acellular Dermal Matrix," *Journal of Tissue Engineering and Regenerative Medicine* 15, no. 12 (2021): 1092–1104.

45. W. Xie, X. Fu, F. Tang, et al., "Dose-Dependent Modulation Effects of Bioactive Glass Particles on Macrophages and Diabetic Wound Healing," *Journal of Materials Chemistry B* 7 (2019): 940–952.

46. T. A. Wynn and L. Barron, "Macrophages: Master Regulators of Inflammation and Fibrosis," *Seminars in Liver Disease* 30 (2010): 245–257.

47. R. Casadei, G. D'Ablaing, 3rd, B. J. Kaplan, and C. P. Schwinn, "A Cytologic Study of Amniotic Fluid," *Acta Cytologica* 17, no. 4 (1973): 289–298.

48. E. Cutz and P. E. Conen, "Macrophages and Epithelial Cells in Human Amniotic Fluid: Transmission and Scanning Electron Microscopic Study," *American Journal of Anatomy* 151, no. 1 (1978): 87–101.

49. O. Tyden, S. Bergstrom, and B. A. Nilsson, "Origin of Amniotic Fluid Cells in Mid-Trimester Pregnancies," *British Journal of Obstetrics and Gynaecology* 88, no. 3 (1981): 278–286.

50. N. G. Lopez, R. Romero, Y. Leng, et al., "The Origin of Amniotic Fluid Monocytes/Macrophages in Women With Intra-Amniotic Inflammation and/or Infection," *Journal of Perinatal Medicine* 47, no. 8 (2019): 822–830.